Vol. 115: 37–46, 2015
doi: 10.3354/dao02870

DISEASES OF AQUATIC ORGANISMS
Dis Aquat Org

Published June 29

Morphological and molecular characterization of *Thelohanellus hoffmanni* sp. nov. (Myxozoa) infecting goldfish *Carassius auratus auratus*

Eva Lewisch[1,*], Hatem Soliman[2], Peter Schmidt[3], Mansour El-Matbouli[1]

[1]Clinical Division of Fish Medicine, University of Veterinary Medicine, 1210 Vienna, Austria
[2]Fish Medicine and Management, Faculty of Veterinary Medicine, Assiut University, 71515 Assiut, Egypt
[3]Institute for Pathology Forensic Veterinary Medicine, University of Veterinary Medicine, Vienna, Austria

ABSTRACT: A new species of the genus *Thelohanellus* Kudo, 1933 (Myxosporea, Bivalvulida) was isolated from the fins of goldfish *Carassius auratus auratus* (Linnaeus 1758). The fish had been imported from China by an Austrian retailer. Nodules from the margins of the fins contained pyriform myxospores with a singular polar capsule. In valvular view, the spores measured 12.2 µm in length and 6.4 µm in width. In sutural view, the thickness was 2.9 µm. The polar capsule measured 4.2 × 3.1 µm and contained a polar filament with 8 to 9 coils. Histological sections showed plasmodia of 0.2 to 4.0 mm diameter with the earlier developmental stages of the parasite in the periphery and the mature spores closer to the center. In the transmission electron microscope examination, the different developmental stages could be observed. Morphological data, host specificity, tissue tropism, and molecular analysis of the small subunit rDNA identify this parasite as a new species of *Thelohanellus*, which we have named *Thelohanellus hoffmanni* sp. nov.

KEY WORDS: Myxozoa · *Thelohanellus* · Transmission electron microscopy · TEM · Molecular analysis · SSU rDNA

INTRODUCTION

The genus *Thelohanellus* Kudo, 1933 (Myxozoa: Myxosporea: Myxobolidae) includes at least 108 species (Zhang et al. 2013). According to Lom & Dykova (2006), these myxozoans are histozoic parasites of freshwater fish. In valvular view, spores are either pyriform or broadly ellipsoidal and are slimmer in sutural view. They have smooth valves and a singular pyriform or subspherical polar capsule with 1 or 2 coils of polar filament. Sporoplasm is binucleate.

Most reported infections with *Thelohanellus* species are from cyprinid fish, with the majority originating from China and India (Chen & Ma 1998, Basu et al. 2006, Zhang et al. 2013). Among them, until recently, only 12 were reported to infect *Carassius auratus* (Chen & Ma 1998). A new species, *T. testudineus*, was recently reported from allogynogenetic gibel carp *Carassius auratus gibelio* (Bloch, 1782) (Liu et al. 2014a). *Thelohanellus* species show high tissue specificity, infecting gills, fins, and skin and visceral organs (Akhmerov 1955). While most members of the genus *Thelohanellus* are not known to cause severe disease and mortalities, some are pathogenic for fish. One of them is *T. hovorkai*, which is the causative agent of hemorrhagic thelohanellosis in common carp *Cyprinus carpio* (Molnár & Kovács-Gayer 1986, Yokoyama et al. 1998). *T. kitauei* is the causative agent of intestinal giant-cystic disease of common carp (Egusa & Nakajima 1981). Several *Thelohanellus* species have been reported to infect skin and fins of a variety of fish (Zhang et al. 2013). Among them, *T. nikolskii* causes deformations and destruction of fin rays of common carp, with no related mortalities (Molnár & Kovács-Gayer 1982) and *T. testudineus* forms tumor-like cysts in the skin of *C.*

*Corresponding author: eva.lewisch@vetmeduni.ac.at

auratus gibelio, with no impact on fish health according to Liu et al. (2014a). In contrast, infection of skin with *T. wuhanensis* caused high mortality in allogynogenetic gibel carp (Liu et al. 2014b).

Given that some *Thelohanellus* species can be problematic in cyprinids, we aimed to identify and characterize a *Thelohanellus* species isolated from the fins of goldfish that had been imported from China.

MATERIALS AND METHODS

Sample origin

Five ruby goldfish *Carassius auratus auratus* (Linnaeus, 1758) with an average length of 10 cm (9.5–10.5 cm) were submitted by an Austrian retailer to the Clinical Division of Fish Medicine, University of Veterinary Medicine, Vienna, Austria, for clinical examination. The fish belonged to a stock of 500 fish, purchased from China, with no further regional specification, and had been subjected to a conventional quarantine. Water quality was within the normal range, and the behavior of the fish was normal. There was no mortality while fish were in quarantine. According to the retailer, about 20% of the purchased fish showed nodules on their fins (Fig. 1).

Gross and microscopic pathology

Fish were subjected to routine parasitological examination of skin and gills as well as pathoanatomical examination. Nodules from the margin of the fins of each affected fish were excised and dissected with a scalpel blade on a microscopic slide. Contents of the nodules were spread on the slide and coverslipped. The specimens were examined using an Olympus BX 53® light microscope (Olympus Austria). For documentation of all microscopic examinations and measurements, an Olympus digital camera DP72 and software cellSense Standard (Olympus Austria) were used. Spore measurements were taken according to Lom & Arthur (1989), including length (n = 40) and width (n = 36) in frontal view as well as thickness in lateral view (n = 11), and length (n = 24) and thickness (n = 26) of the polar capsule. Measurements are given as mean length ± SD (range) × mean width ± SD (range). Specimens were fixed in 10% neutral buffered formalin and subjected to histological examination, using standard methods for embedding the samples in paraffin, cutting, and staining with hematoxylin and eosin (H&E).

Transmission electron microscopic examination

Samples of fin clips with nodules were fixed in 5% glutaraldehyde for 4 h at 4°C. Subsequently, samples were washed twice with 0.2 M phosphate-buffered saline, pH 7.4, incubated overnight in the same buffer at 4°C and then post-fixed in 1% osmium tetroxide. After several steps of dehydration, the tissues were embedded in Epon. Semi-thin sections were cut and stained with toluidine blue. Ultra-thin sections were contrasted with uranyl acetate and lead citrate and then examined under an electron microscope (Zeiss EM 109, 50 kV).

Molecular analysis

DNA extraction

Nodules filled with spores were collected from the infected fins and subjected to DNA extraction using

Fig. 1. Goldfish *Carassius auratus auratus*, showing multiple nodules on the margins of the fins filled with *Thelohanellus hoffmanni* sp. nov. spores. Nodules appeared white, gray, or black and were arranged in grape-like clusters

the QIAamp DNA Mini Kit for tissue (Qiagen). Spores were disrupted and homogenized with stainless steel beads (5 mm; Qiagen) for 1 min at 30 Hz in 180 µl lysis buffer using a Qiagen Tissue Lyser II. Following disruption, the samples were incubated with Proteinase K and lysis buffer at 56°C until complete lysis. DNA extraction was then completed as per the manufacturer's instructions and eluted in 100 µl elution buffer. A negative extraction control was performed to control contaminations during the extraction process. Quality and quantity of the purified DNA was assessed by measuring the optical density at 260 and 280 nm. DNA samples were stored in aliquots at –20°C.

Small subunit ribosomal DNA amplifications

The small subunit ribosomal DNA (SSU rDNA) of the suspected myxosporean parasite was first amplified with the universal eukaryotic primers ERIB1 and ERIB10 (Barta et al. 1997, Fiala 2006). Subsequently, a nested PCR reaction was carried out using myxosporean-specific SSU rDNA primers (MyxospecF and MyxospecR) according to Fiala (2006) with some modifications. Briefly, amplification was performed in a 25 µl reaction volume with 2× ReddyMix PCR Master mix (Thermo Scientific) which contained 75 mM Tris-HCl (pH 8.8), 20 mM $(NH_4)_2SO_4$, 1.5 mM $MgCl_2$, 0.01% Tween-20, 0.2 mM each nucleotide triphosphate, 1.25 U thermoprime plus DNA polymerase, red dye for electrophoresis, 3 µl of DNA template, and 10 pmol of each primer. The amplification was carried out in a Mastercycler Gradient thermocycler (Eppendorf) with the following cycling profile: 95°C for 3 min, then 35 PCR cycles of 95°C for 1 min (denaturation), 48°C for 1 min (annealing), and 72°C for 2 min (extension), with a final extension step of 72°C for 10 min. Two µl from the initial PCR were used as a template for the nested PCR using 10 pmol each of MyxospecF and MyxospecR primers. PCR conditions were the same as in the first round, but with an annealing temperature of 52°C.

Detection and sequencing of the PCR products

PCR amplification products were subjected to electrophoresis on 1.5% agarose in Tris acetate–EDTA buffer (0.04 M Tris acetate, 1 mM EDTA), stained with ethidium bromide, and visualized on a UV transilluminator. A 100 bp ladder (Invitrogen) was used to comparatively determine the length of the PCR amplicons. For sequencing, the PCR products were separated from the agarose gel, excess primers, and unincorporated nucleotides, using the MinElute gel extraction kit (Qiagen) according to the manufacturer's instructions. Purified PCR product concentrations were determined by spectrophotometry. PCR products were sequenced in a commercial sequencing laboratory (LGC Genomics, Berlin, Germany) using the Myxospec-F primer.

Phylogenetic analysis

Obtained sequences were subjected to Basic Local Alignment Search Tool (BLAST) analysis to search GenBank for homologous nucleotide sequences and to determine whether the sequences were of host or parasite origin (Altschul et al. 1997). Sequences (26 *Thelohanellus* species and 12 other myxozoan taxa) were downloaded from GenBank for the phylogenetic analysis. Multiple sequence alignments were generated using the default settings of Clustal W (Thompson et al. 1997). A phylogenetic tree based on the SSU rDNA sequences was constructed using the maximum likelihood (ML) method in the MEGA6 software, with bootstrap confidence values calculated using 1000 replicates (Tamura et al. 2013). *Sphaerospora renicola* (GenBank accession number JF758875) was used as the outgroup. The outgroup was selected based on obscure relationships between outgroup and ingroup taxa (Sanderson & Shaffer 2002, Cameron et al. 2004). *S. renicola* is closely related to the other groups but less closely related than any single one of the other groups to each other.

RESULTS

Clinical findings

Four out of the 5 sampled fish had nodules of up to 4 mm in diameter on the margins of their fins. Nodules were white, gray, or black and arranged in grape-like clusters (Fig. 1). No specific fin types were more likely to be infected than any others, and all were heavily infected. In some cases, the fins showed hyperemia and increased formation of blood vessels. No other signs of disease, based solely on gross examination of the fish, could be observed.

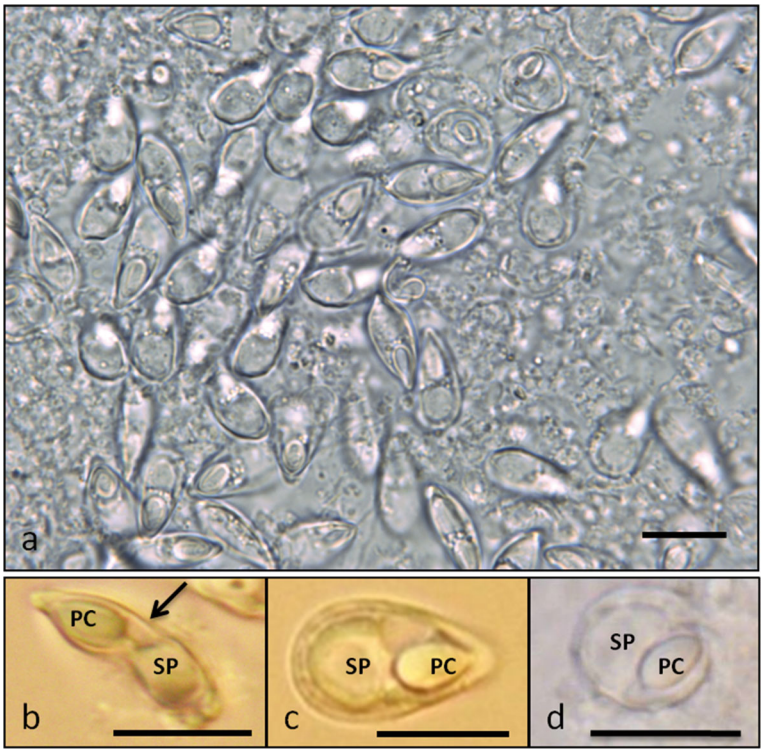

Fig. 2. (a) Wet mount of a nodule, showing fresh spores of *Thelohanellus hoffmanni* sp. nov. The mature spores appeared pyriform with tapering anterior and round posterior ends. (b) Lateral view showing the suture (arrow) and valves. (c) Frontal view showing the polar capsule and the sporoplasm. (d) Atypical round spore. SP: sporoplasm; PC: polar capsule. Scale bars = 10 µm

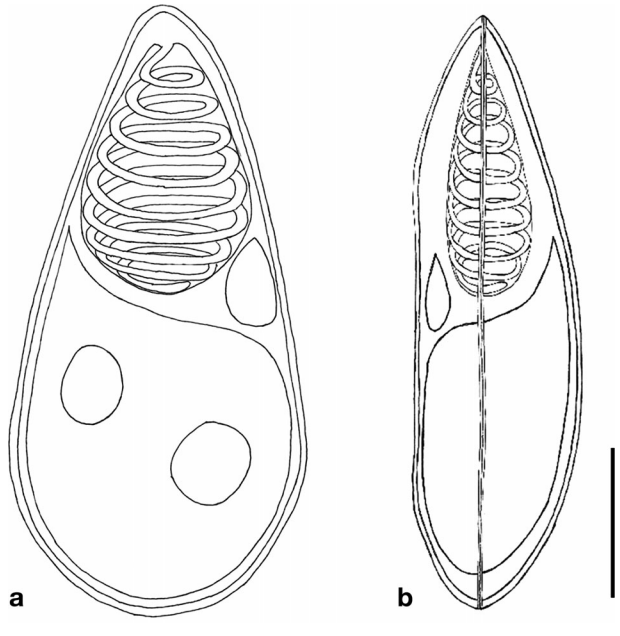

Fig. 3. Schematic of the spore of *Thelohanellus hoffmanni* sp. nov. from goldfish *Carassius auratus auratus* observed in (a) frontal and (b) lateral view, showing the binucleated sporoplasm and the coils of the polar filaments; scale bar = 3 µm

Wet mounts and spore morphology

After rupturing one of the nodules, free spores were observed under the microscope (Fig. 2). Microscopic examination of the spores suggested that this parasite belongs to the class Myxosporea, family Thelohanellidae, genus *Thelohanellus* according to the classification proposed by Lom & Dykova (2006). The mature spores were pyriform with tapering anterior and round posterior ends (Fig. 2). In valvular view, they measured 12.2 ± 0.7 (11.0–14.1) µm in length and 6.4 ± 0.6 (5.3–7.6) µm in width. In the lateral view, spores appeared only slightly curved with a thickness of 2.9 ± 0.7 (2.4–4.0) µm (Fig. 2b). A single pyriform polar capsule was situated on the acuminated end of the spore. The polar capsule itself measured 4.2 ± 0.5 × 3.1 ± 0.4 (3.3–5.1 × 2.3–3.9) µm and contained the polar filament, which was coiled in 8 to 9 turns (Fig. 3, see also Fig. 5d). The binucleated sporoplasm was situated at the rounded end of the spore. The suture of the spore, which was elongated in relation to the body, could readily be identified. Atypical round spores were also occasionally found in a smear of ruptured nodules (Fig. 2d)

Histological examination

Histological sections showed layers of the skin with a few developing parasites in the epidermis and dermis and an increased number of melanocytes in the dermis (Fig. 4), when compared to uninfected fish. Although some fins had macroscopically shown hyperemia and increased formation of blood vessels, there was no sign of inflammation in the histological sections. Large plasmodia (0.2 to 4.0 mm diameter) could be seen between the dermal layers of the fins (Fig. 4). The wall of the plasmodium consisted of eosinophilic tissue with an inner monolayer of flat cells (Fig. 4). On the inner side of this plasmodium wall, from the periphery to the center, fluffy eosinophilic masses, followed by developmental stages of the spores could be seen. Early developmental stages were situated in the periphery, whereas maturing and mature spores were located in the center of the plasmodium (Fig. 4).

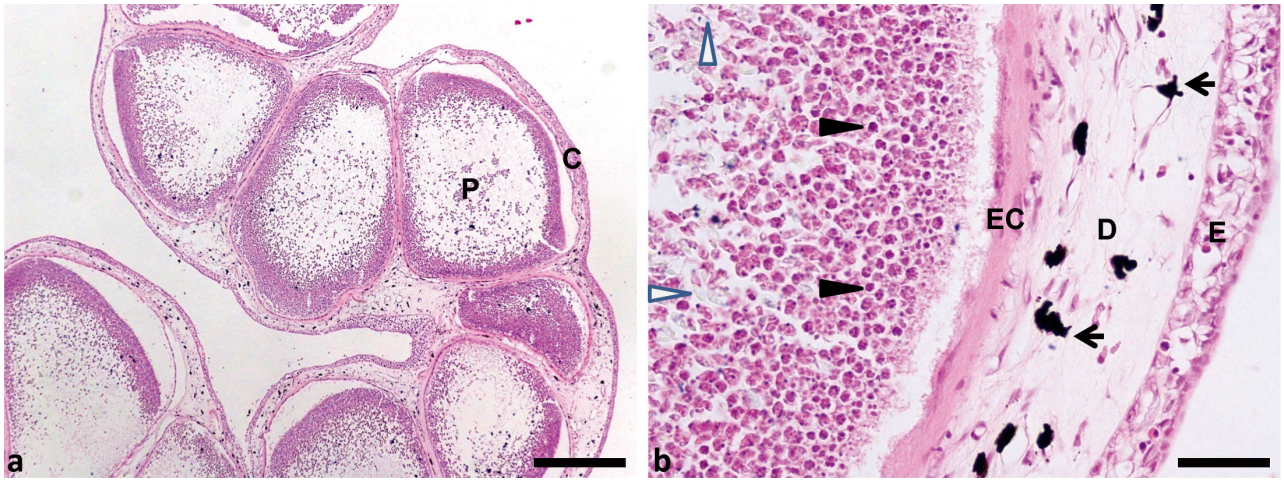

Fig. 4. Histopathology of the caudal fin of goldfish *Carassius auratus auratus* with nodules (plasmodia) as seen in Fig. 1, H&E stain. (a) Plasmodia (P) are filled with different developmental stages of *Thelohanellus hoffmanni* sp. nov.; C: cyst wall; scale bar = 500 µm. (b) Higher magnification of a nodule from (a); D: dermis; E: epidermis; EC: eosinophilic cyst wall. Melanocytes (arrows) are gathering together around the plasmodia. Note that the early developmental stages are in the periphery of the plasmodium (black arrowheads), and the mature spores are in the center (white arrowheads); scale bar = 50 µm

Transmission electron microscopy (TEM)

Ultrathin sections of heavily infected fins showed that the peripheral ectoplasmic zone of the plasmodium contained early developmental stages with non-differentiated stages and more cell stages (Fig. 5a). Extending into the central region of the plasmodium were various stages of sporogenesis, which followed the pattern similar to that in many other myxosporeans with sporoblast formation (Fig. 5b). Sporogonic cells divided to form a group of closely adhering cells, later transforming into capsulogenic, valvogenic, and sporoplasmic cells. In young sporoblasts, the development of the second capsulogenic cell was abortive, resulting in the formation of a single polar capsule (Fig. 5c,d) in each of the 2 spores in the pansporoblast (Fig. 5e). The morphogenesis of the capsulogenic cells corresponded to that of most other myxosporeans. The external tube was withdrawn into the capsule, and the mouth of the mature polar capsule was plugged by a corklike stopper. Posterior to the capsulogenic cell was a typical binucleate sporoplasm cell (Fig. 5e) surrounded by irregular dense matrix and numerous sporoplasmosomes. A schematic illustration of the spore, based on light microscopy and TEM observations, is shown in Fig. 3.

Molecular investigation

Myxosporean-specific SSU rDNA primers were used to amplify a single 852 bp amplicon from each sample examined. No amplification products were detected from the negative extraction or no-template controls. Alignment of the sequences obtained from the PCR products revealed 100% similarity between each other. A BLAST search of the amplified sequence against the GenBank database revealed 93% similarity to the SSU rDNA of *T. testudineus*, 92% similarity to that of *T. wuhanensis*, 91% similarity to that of *T. hovorkai*, and 91% similarity to that of *T. kitauei.* A phylogenetic tree of these results is shown in Fig. 6. The sequence obtained from this study was deposited in GenBank under accession number KJ820997.

Taxonomic summary

Name: *Thelohanellus hoffmanni* sp. nov.
Type host: goldfish *Carassius auratus auratus*
Life stage infected: adult
Geographic locality: China; no further details available
Site of infection: dorsal, caudal, pectoral, abdominal, anal fins
Prevalence: 20%
Specimens deposited: under No. 12/06941 in the collection of the Clinical Division of Fish Medicine, University of Veterinary Medicine, Vienna, Austria
GenBank accession number: KJ820997
Etymology: The species was named for Prof. Rudolph Hoffmann in recognition of his support and contribution to myxozoan research

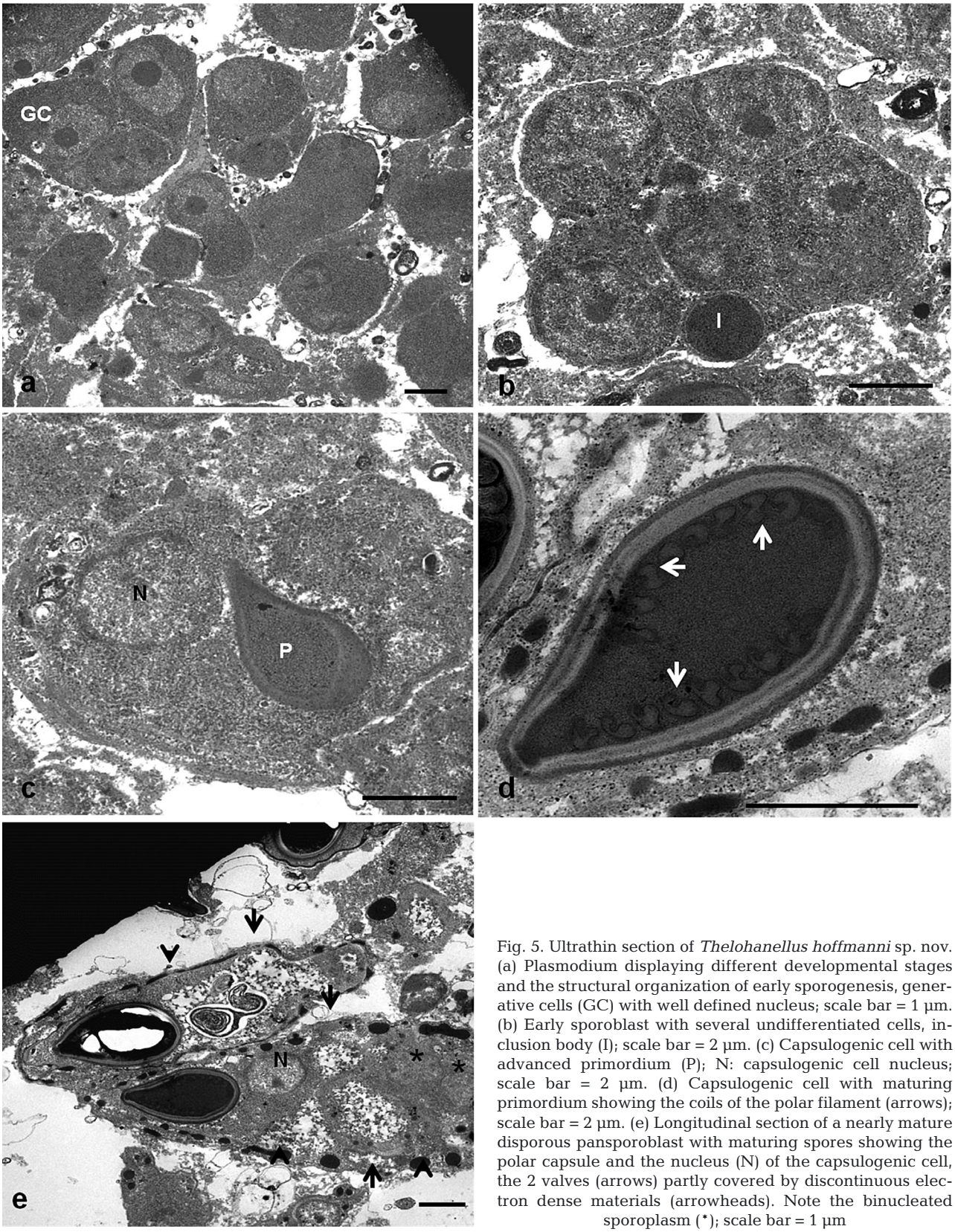

Fig. 5. Ultrathin section of *Thelohanellus hoffmanni* sp. nov. (a) Plasmodium displaying different developmental stages and the structural organization of early sporogenesis, generative cells (GC) with well defined nucleus; scale bar = 1 µm. (b) Early sporoblast with several undifferentiated cells, inclusion body (I); scale bar = 2 µm. (c) Capsulogenic cell with advanced primordium (P); N: capsulogenic cell nucleus; scale bar = 2 µm. (d) Capsulogenic cell with maturing primordium showing the coils of the polar filament (arrows); scale bar = 2 µm. (e) Longitudinal section of a nearly mature disporous pansporoblast with maturing spores showing the polar capsule and the nucleus (N) of the capsulogenic cell, the 2 valves (arrows) partly covered by discontinuous electron dense materials (arrowheads). Note the binucleated sporoplasm (*); scale bar = 1 µm

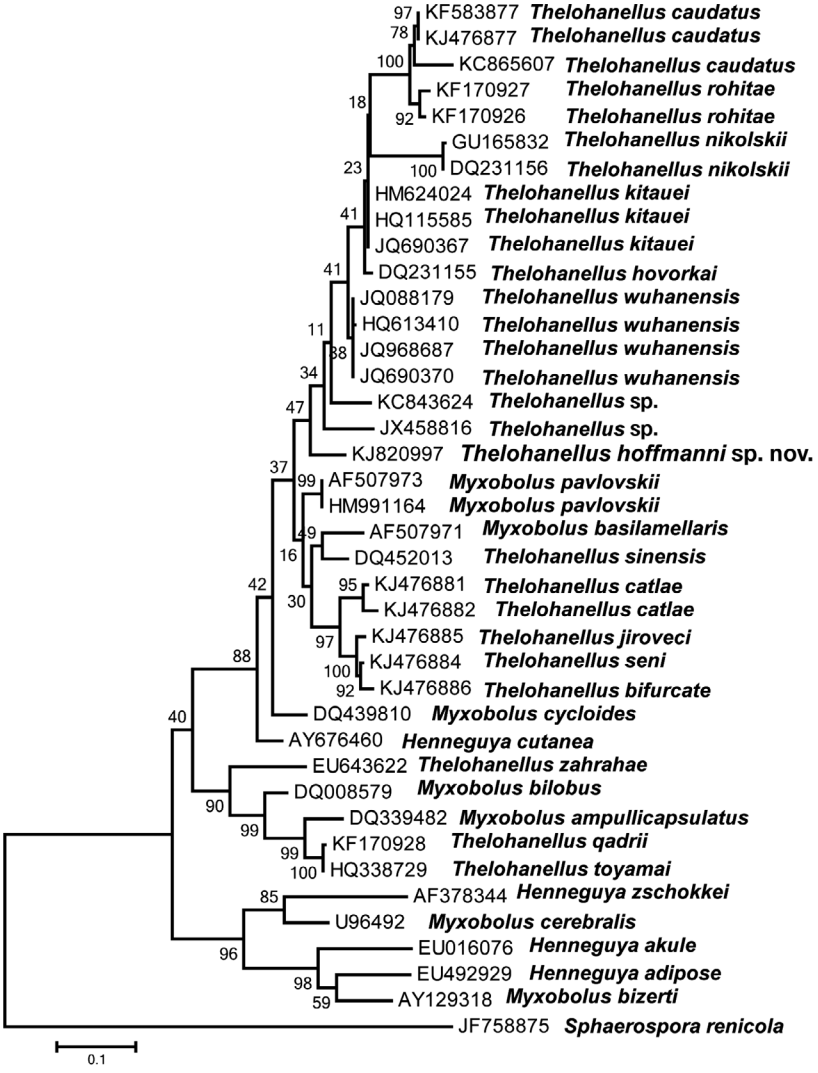

Fig. 6. Phylogenetic tree demonstrating the relative positions of *Thelohanellus hoffmanni* sp. nov. to other myxosporidian species. The tree is based on the nucleotide sequences of the small subunit ribosomal DNA (SSU rDNA) of myxosporidian species that are deposited in GenBank. The tree was generated using the maximum likelihood (ML) method using MEGA 6 software. Numbers at nodes indicate bootstrap confidence values calculated using 1000 replicates. GenBank accession numbers are listed beside the species names. The tree was oriented by using the SSU rDNA sequence of *Sphaerospora renicola* as the outgroup

Plasmodia: nodular, up to 4 mm, white, gray, or black, arranged in grape-like clusters on the margins of the fins, containing different developmental stages of spores

Remarks: According to the descriptions given by Zhang et al. (2013); spore morphology of several *Thelohanellus* species reported from *Carassius auratus* resembles *T. hoffmanni* sp. nov. (see Table 1). Nevertheless, size of spores in all of these species differs substantially from those of *T. hoffmanni* sp. nov., with *T. hupehensis* (Nie & Li 1992) being the closest, but infecting gills, spleen, and kidney. None of the described *Thelohanellus* species of *Carassius auratus* is reported to infect the fins, while some of them have been reported in the skin (*T. liaohoensis* Chen & Ma 1998, *T. parasagittarius* Chen & Ma 1998, *T. testudineus* Liu et al. 2014a, *T. wuhanensis* Xiao & Chen 1993). Spores of *T. liaohoensis* and *T. parasagittarius* are distinctly longer (*T. liaohoensis*: range 20.4–21.8 µm; *T. parasagittarius*: range: 22.8–24.6 µm; Chen & Ma 1998) and also differ in shape (both are elongate-ovoidal in valvular view) from those of *T. hoffmanni* sp. nov.; those of *T. testudineus* and *T. wuhanensis* are similar in shape, but larger in size (see Table 1). Based on these differences in spore morphology and site predilection we propose a new species of *Thelohanellus*.

DISCUSSION

In this study, we describe a new myxozoan parasite that belongs to the genus *Thelohanellus* and infects fins of goldfish. Depending on environmental conditions and host, myxozoan parasite spores can display variations in morphological features. Such environmental changes can enable infection of new species or new sites (Urawa et al. 1995). Thus, our conclusions were based on comparing available data from various *Thelohanellus* species. These data included hosts, predilection site, spore morphological and metric characteristics, as well as molecular investigations.

In goldfish and gibel carp, several *Thelohanellus* species have been reported (Chen & Ma 1998, Zhang et al. 2013). Most of them were reported from China (Chen & Ma 1998), whereas *T. carassii* was found in far-east Russia (Akhmerov 1960). In 1 case, an infection with a *Thelohanellus* sp. in goldfish was documented in Japan (Yokoyama et al. 1991). In that case, the authors described the detection of *Thelohanellus* sp., without further specifications, in the minced body parts, excluding visceral organs. In our study, affected fish had been imported from China, in

Table 1. *Thelohanellus hoffmanni* sp. nov. and morphologically similar species of the genus *Thelohanellus*. *Thelohanellus* species were included based on host (goldfish *Carassius auratus*), with the addition of *T. nikolskii* due to similar appearance on fins. A second criterion was morphology of spores. nd: no data; SSU sim.: % similarity of SSU rDNA to that of *T. hoffmanni* sp. nov. (GenBank accession numbers are given where available)

Thelohanellus species	Infecting		Dimensions in µm (range, mean [±SD])				Polar filament coils	SSU sim. (%)	GenBank acc. no(s).	Reference
	Host	Organ(s)	Spore			Polar capsule				
			Length	Width	Thickness	Length	Width			
T. carassii	*C. a. gibelio*	Gills	16.0–18.0, nd	10.0–10.5, nd	nd, nd	7.5–8.0, nd	5.4–6.0,	nd nd	nd	–	Akhmerov (1960)
T. hupehensis	*C. a. auratus*	Gill, spleen, kidney	14.0–16.5, nd	8.4–9.6, nd	nd, 8	6.4–7.2, nd	2.5–3.0, nd	nd	nd	–	Nie & Li (1992)
T. nanhaiensis	*C. a. auratus*	Gill	15.6–18.0, 17.0	9.6–10.8, 10.0	7.4–8.2, 7.8	8.2–9.6, 8.9	4.6–5.8, 5.1	6–7	nd	–	Chen & Ma (1998)
T. relortus	*C. a. auratus*	Gill	15.0–17.4, 16.4	9.5–9.8, 9.6	8.4–8.6, 8.5	6.2–7.4, 7.0	4.2–4.8, 4.6	8–9	nd	–	Chen & Ma (1998)
T. testudineus	*C. a. gibelio*	Skin	18.6–20.8, 19.7±0.7	6.6–8.4, 7.6±0.4	6.6–8.8, 7.3±0.5	10.0–11.9, 11.1±0.5	4.3–5.8, 5.3±0.3	7–8	93	KC843642	Liu et al. (2014a)
T. nikolskii	*Cyprinus carpio*	Fins	17–18.5, 17.5	10–11, 10.5	8.3–8.7, 8.5	6.5–7.0, 6.8	5.1–6.2, 5.5	7 (outer), 2 (inner)[a]	84	GU165832, DQ231156	Molnár & Kovacs-Gayer (1982)
T. wuhanensis	*C. a. gibelio*	Skin	21.9–26.9, 24.5	11.4–15.5, 13.7	10.8–14.1, 11.8	9.6–12.8, 11.5	8.1–10.3, 9.1	7–10			Xiao & Chen (1993)
			21.8–24.0, 22.9±0.6	12.2–14.3, 13.3±0.5	9.9–11.6, 10.6±0.5	9.6–11.9, 10.8±0.6	7.5–9.7, 8.6±0.5	8–10	92	JQ968687	Liu et al. (2014b)
T. hoffmanni sp. nov.	*C. a. auratus*	Fins	11.0–14.1, 12.2±0.7	5.3–7.6, 6.4±0.6	2.4–4.0, 2.9±0.7	3.3–5.1, 4.2±0.5	2.3–3.9, 3.1±0.4	8–9	100	KJ820997	Present study

[a]Data for polar filament coils from Antychowicz et al. (2005)

accordance with most *Thelohanellus* cases reported from *Carassius auratus*.

Species from different genera of myxosporean parasites have been recorded from fins. Among them, *Myxobolus diversus* has been described from goldfish, with localization and size of plasmodia similar to the present case (Molnár & Székely 2003). Of the 108 nominative species of *Thelohonellus* summarized by Zhang et al. (2013), 14 infect fins of fish; most of these were described from cyprinid fish in India, Cameroon, or eastern Asia. Despite some similarities in spore morphology and size to *T. hoffmanni* sp. nov., none shows accordance in the whole profile. This is also true for *T. nikolskii*, which causes lesions very similar to the present case. Infection with *T. nikolskii* is well documented in carp in wide parts of Europe and Asia (Jeney 1979, Molnár & Kovács-Gayer 1982, Moshu & Molnár 1997). Nevertheless, pseudocysts of *T. nikolskii* are not located exclusively on the margins of the fins, as in the examined goldfish, but on the whole surface. Molnár (2002) examined common carp, koi carp, and goldfish for the presence of *T. nikolskii*, finding common carp, and, to a lesser degree, koi carp infected with the parasite. *T. nikolskii* could not be found in goldfish, which were reared in ponds next to the common carp, leading to the conclusion that susceptibility of fish and species specificity of the parasite were the reasons for this finding (Molnár 2002). Moreover, in the described *T. hoffmanni* sp. nov., the size of the spores and the number of turns of the polar filament did not match *T. nikolskii.* In the present case, spores were smaller and the polar filament was coiled in 8 or 9 turns, in contrast to 7 or 8 turns in *T. nikolskii*.

To date, no reports are available on *Thelohanellus* species infecting the fins of *C. auratus*, while infection of the skin was demonstrated in several cases (*T. parasagittarius*: Chen & Ma 1998; *T. liaohoensis*: Chen & Ma 1998;

T. wuhanensis: Xiao & Chen 1993; *T. testudineus*: Liu et al. 2014a). Besides the different site specificities, there are also substantial differences in shape and size of the species mentioned compared to *T. hoffmanni* sp. nov.

The spore morphology of *T. hoffmanni* sp. nov. was compared with *Thelohanellus* species reported from *C. auratus* (Table 1). Morphological similarity of spores could be demonstrated for *T. carassii*, *T. hupehensis*, *T. nanhaiensis*, *T. relortus*, *T. testudineus*, and *T. wuhanensis*, showing a tapered anterior and a rounded posterior end. Nevertheless, all of these spores were of a larger size compared to spores of *T. hoffmanni* sp. nov., with *T. hupehensis* being closest in spore size. Of the mentioned *Thelohanellus* species, morphological descriptions of polar capsules of *T. carassii*, *T. hupehensis*, and *T. testudineus* match that of the new species described herein, but again, they are distinctly larger and occupy half of the spore in the case of *T. testudineus* and *T. hupehensis*, in contrast to our findings (Table 1).

Sporogenesis of *T. hoffmanni* sp. nov. followed the general pattern of most ultrastructurally studied myxobolids. The asynchronous division of secondary and tertiary cells and asynchronous development in spore formation of *T. hoffmanni* sp. nov. resembled the disporous *Thelohanellus* and *Myxobolus* species (El-Matbouli et al. 1990, Lom & Dykova 1992). Mature spores of *T. hoffmanni* sp. nov. have a binucleated sporoplasm. This feature has been reported in all ultrastructurally described *Thelohanellus* species (Lom & Dykova 1992, Azevedo et al. 2011). Capsulogenesis is thought to proceed along the pattern observed in most myxosporeans and described by Lom & Puytorac (1965). The capsulogenic cells in early sporoblasts of *T. hoffmanni* sp. nov. had large amounts of rough endoplasmic reticulum, but little Golgi apparatus. This is in accordance with similar observations in various other myxosporeans (Current & Janovy 1978, Desser & Paterson 1978, Desportes & Théodoridès 1982, Lom et al. 1985, Davies & Sienkowski 1988, Sitjà-Bobadilla & Alvarez-Pellitero 1993, El-Matbouli & Hoffmann 1994).

Concerning molecular findings, the most closely related species was *T. testudineus* (Fig. 6, accession number KC843624), with 93% similarity of the SSU rDNA, followed by *T. wuhanensis* with 92%. Both those species infect skin of allogynogenetic gibel carp (Chen & Ma 1998, Zhu et al. 2012, Liu et al. 2014a,b). These sequence differences are outside what is typically considered conspecific for myxozoans (Liu et al. 2010). Phylogenetic analysis in the present study showed *T. hoffmanni* sp. nov. clustered with *Thelohanellus* species that infect fins and skin, such as *T. nikolskii*, *T. rohitae*, *T. caudatus*, and *T. wuhanensis.* Nevertheless, clinical signs, spore morphology, and species preference of *T. testudineus* and *T. wuhanensis* differed substantially from our findings (Table 1).

In conclusion, the investigated member of Myxobolidae described in this study clearly belongs to the genus *Thelohanellus*. The morphological and morphometric characters as well as the molecular genetics data indicate a novel species for which we propose the species name *Thelohanellus hoffmanni* sp. nov.

Acknowledgements. We thank N. Dinhopl for assistance with the TEM. This work was funded in part by the Clinical Division of Fish Medicine and the University of Veterinary Medicine, Vienna.

LITERATURE CITED

Akhmerov AK (1955) Paths of species formation in Myxosporidia of the genus *Thelohanellus kudo* from the Amur carp. Dokl Akad Nauk SSSR 105:1129–1131 (In Russian)

Akhmerov AK (1960) Myxosporidia of fishes from the Amur River basin. Rybnoe Khozyaistvo Vnutrennykh Vodoemov Latvijskoi SSR 5:240–307 (in Russian)

Altschul SF, Madden TL, Schäffer AA, Zhang J, Zhang Z, Miller W, Lipman DJ (1997) Gapped BLAST and PSI-BLAST: a new generation of protein database search programs. Nucleic Acids Res 25:3389–3402

Antychowicz J, Matras M, Reichert M, Kramer I (2005) Preliminary observation on epizootiology and pathogenesis of *Thelohanellus nikolskii* infection in carp in Poland. Bull Vet Inst Pulawy 49:403–406

Azevedo C, Samuel N, Saveia AP, Delgado F, Casal G (2011) Light and electron microscopical data on the spores of *Thelohanellus rhabdalestus* n. sp. (Myxozoa: Myxosporea), a parasite of a freshwater fish from the Kwanza River, Angola. Syst Parasitol 78:19–25

Barta JR, Martin DS, Liberator PA, Dashkevicz M and others (1997) Phylogenetic relationships among eight *Eimeria* species infecting domestic fowl inferred using complete small subunit ribosomal DNA sequences. J Parasitol 83: 262–271

Basu S, Modak BK, Haldar DP (2006) Synopsis of the Indian species of the genus *Thelohenellus* Kudo, 1933 along with the description of *Thelohenellus disporomorphus* sp. n. J Parasitol Appl Anim Biol 15:81–94

Cameron SL, Miller KB, D'Haese CA, Whiting MF, Barker SC (2004) Mitochondrial genome data alone are not enough to unambiguously resolve the relationships of Entognatha, Insecta and Crustacea *sensu lato* (Arthropoda). Cladistics 20:534–557

Chen QL, Ma CL (1998) Myxozoa, Myxosporea. Fauna Sinica. Science Press, Beijing

Current WL, Janovy J (1978) Comparative study of ultrastructure of intralamellar types of *Henneguya exilis* Kudo from channel catfish. J Protozool 25:56–65

Desportes I, Théodoridès J (1982) Données ultrastructurales sur la sporogenèse de deux Myxosporidies rapportées

aux genres *Leptotheca* et *Ceratomyxa* parasites de *Merluccius merluccius* (L.) (Téléostéen Merluciidae). Protistologica 18:533–557

Davies AJ, Sienkowski IK (1988) Further studies on *Zschokkella russelli* Tripathi (Myxozoa: Myxosporea) from *Ciliata mustela* L. (Teleostei: Gadidae), with emphasis on ultrastructural pathology and sporogenesis. J Fish Dis 11:325–336

Desser SS, Paterson B (1978) Ultrastructural and cytochemical observations on sporogenesis of *Myxobolus* sp. (Myxosporidia: Myxobolidae) from the common shiner *Notropis cornutus.* J Protozool 25:314–326

Egusa S, Nakajima K (1981) A new myxozoa *Thelohanellus kitauei*, the cause of intestinal giant cystic disease of carp. Fish Pathol 15:213–218

El-Matbouli M, Hoffmann RW (1994) *Sinuolinea tetraodoni* n. sp., a myxosporean parasite of freshwater pufferfish *Tetraodon palembangensis* from Southeast Asia — light and electron microscope observations. Dis Aquat Org 19: 47–54

El-Matbouli M, Fischer-Scherl T, Hoffmann RW (1990) Light and electron microscopic studies on *Myxobolus cotti* El-Matbouli and Hoffmann, 1987 infecting the central nervous system of bullhead (*Cottus gobio*). Parasitol Res 76: 219–227

Fiala I (2006) The phylogeny of Myxosporea (Myxozoa) based on small subunit ribosomal RNA gene analysis. Int J Parasitol 36:1521–1534

Jeney G (1979) The occurrence of *Thelohanellus dogielei* Achmerov 1955 (Myxosporidia) on carp (*Cyprinus carpio*) in fish ponds in Hungary. Parasitol Hung 12:19–20

Liu Y, Gu ZM, Luo YL (2010) Some additional data to the occurrence, morphology and validity of *Myxobolus turpisrotundus* Zhang, 2009 (Myxozoa: Myxosporea). Parasitol Res 107:67–73

Liu Y, Jia L, Huang MJ, Gu ZM (2014a) *Thelohanellus testudineus* n. sp. (Myxosporea: Bivalvulida) infecting the skin of allogynogenetic gibel carp *Carassius auratus gibelio* (Bloch) in China. J Fish Dis 37:535–542

Liu Y, Yuan J, Jia L, Huang M, Zhou Z, Gu Z (2014b) Supplemental description of *Thelohanellus wuhanensis* Xiao & Chen, 1993 (Myxozoa: Myxosporea) infecting the skin of *Carassius auratus gibelio* (Bloch): ultrastructural and histological data. Parasitol Int 63:489–491

Lom J, Arthur JR (1989) A guideline for preparation of species descriptions in Myxosporea. J Fish Dis 12:151–156

Lom J, Dykova I (1992) Myxosporidia (Phylum Myxozoa). In: Lom J, Dykova I (eds) Protozoan parasites of fishes: developments in aquaculture and fisheries science, Vol 26. Elsevier, Amsterdam, p 159–235

Lom J, Dykova I (2006) Myxozoan genera: definition and notes on taxonomy, life-cycle terminology and pathogenic species. Folia Parasitol 53:1–36

Lom J, Puytorac P (1965) Studies on the myxosporidian ultrastructure and polar capsule development. Protistologica 1:53–65

Lom J, Körting W, Dyková I (1985) Light and electron microscope redescription of *Sphaerospora tincae* Plehn, 1925 and *S. galinae* Evlanov, 1981 (Myxosporea) from the tench, *Tinca tinca* L. Protistologica 21:487–497

Molnár K (2002) Differences between the European carp (*Cyprinus carpio carpio*) and the coloured carp (*Cyprinus carpio haematopterus*) in susceptibility to *Thelohanellus nikolskii* (Myxosporea) infection. Acta Vet Hung 50:51–57

Molnár K, Kovács-Gayer E (1982) Occurrence of two species of *Thelohanellus* (Myxosporea: Myxozoa) of Far-Eastern origin in common carp populations of the Hungarian fish farms. Parasitol Hung 14:51–55

Molnár K, Kovács-Gayer E (1986) Biology and histopathology of *Thelohanellus hovorkai* Akhmerov 1960 (Myxosporea, Myxozoa), a protozoan parasite of the common carp (*Cyprinus carpio*). Acta Vet Hung 34:67–72

Molnár K, Székely C (2003) Infection in the fins of the goldfish *Carassius auratus* caused by *Myxobolus diversus* (Myxosporea). Folia Parasitol 50:31–36

Moshu A, Molnár K (1997) Thelohanellus (Myxozoa: Myxosporea) infection of the scales in the European wild carp *Cyprinus carpio carpio.* Dis Aquat Org 28:115–123

Nie DS, Li LX (1992) On the Myxosporidians of freshwater fishes from Lake Huama, Hubei Province: descriptions of new species (Myxosporea: Bivalvulida). Acta Zootaxonom Sin 17:133–146 (in Chinese with English abstract)

Sanderson MJ, Shaffer HB (2002) Troubleshooting molecular phylogenetic analysis. Annu Rev Ecol Syst 33:49–72

Sitjà-Bobadilla A, Alvarez-Pellitero P (1993) *Zschokkella mugilis* n. sp. (Myxosporea: Bivalvulida) from mullets (Teleostei: Mugilidae) of Mediterranean waters: light and electron microscopic description. J Eukaryot Microbiol 40:755–764

Tamura K, Stecher G, Peterson D, Filipski A, Kumar S (2013) MEGA6: molecular evolutionary genetics analysis version 6.0. Mol Biol Evol 30:2725–2729

Thompson JD, Gibson TJ, Plewniak F, Jeanmougin F, Higgins DG (1997) The Clustal-X windows interface: flexible strategies for multiple sequence alignment aided by quality analysis tools. Nucleic Acids Res 25:4876–4882

Urawa S, Yokoyama H, Kent ML, Margolis L (1995) Geographical variation in morphology and host susceptibility in actinosporeans of *Myxobolus arcticus.* 4th International Symposium on Fish Parasitology, Oct 3–7, University of Munich (abstract)

Xiao CX, Chen QL (1993) Two new Myxosporidia (Protozoa) from freshwater fish in Hubei province. Trans Res Fish Dis 1:83–84 (in Chinese)

Yokoyama H, Ogawa K, Wakabayashi H (1991) A new collection method of actinosporeans — a probable infective stage of myxosporeans to fishes — from tubificids and experimental infection of goldfish with the actinosporean, *Raabeia* sp. Fish Pathol 26:133–138

Yokoyama H, Liyanage YS, Sugai A, Wakabayashi H (1998) Hemorrhagic thelohanellosis of color carp caused by *Thelohanellus hovorkai* (Myxozoa: Myxosporea). Fish Pathol 33:85–89

Zhang JYZ, Gu ZM, Kalavati C, Eiras JC, Liu Y, Guo QY, Molnár K (2013) Synopsis of the species of *Thelohanellus* Kudo, 1933 (Myxozoa: Myxosporea: Bivalvulida). Syst Parasitol 86:235–256

Zhu YT, Lu HD, Cai SJ (2012) Redescription of *Thelohanellus wuhanensis* Xiao et Chen, 1993 (Myxozoa, Myxosporea) infecting allogynogenetic crucian carp (*Carassius auratus gibelio*) and phylogenic analysis based on 18S rDNA sequence. Acta Zootaxonom Sin 37:681–688

Editorial responsibility: Dieter Steinhagen, Hannover, Germany

Submitted: July 10, 2014; Accepted: March 27, 2015
Proofs received from author(s): June 8, 2015